IOSR Journal of Mechanical and Civil Engineering (IOSR-JMCE)
e-ISSN: 2278-1684,p-ISSN: 2320-334X, Volume 16, Issue 1 Ser. III (Jan. - Feb. 2019), PP 38-52
www.iosrjournals.org

Numerical Study of In-cylinder Combustion Characteristics and Emission of Hydrogen IC Engine using a 3D Model with Chemical Kinetics

Hassan A. Khairallah[1] and Umit O. Koylu[2]
[1]*Department of Mechanical Engineering, Tobruk University , Tobruk, Libya.*
[2]*Department of Mechanical andAerospace Engineering, Missouri University of Science and Technology, Rolla, MO 65401 USA.*
Corresponding Author: Hassan A. Khairallah

Abstract: *During the past decade, considerable effort has been made to introduce alternative energy sources for use in conventional diesel and gasoline engines. Many researchers have attempted to use hydrogen as a fuel in the diesel engine due to its ability to reduce pollutant emissions, such as carbon monoxide and unburned hydrocarbons. With the rapid increase in computational capabilities, 3D computational fluid dynamics CFD codes become essential tools for practical design, control and optimization of hydrogen engines. In the present study, detailed chemical kinetic reactions with twenty nine steps of hydrogen oxidation with additional nitrogen oxidation reactions were coupled with AVL FIRE® code to study combustion processes in a diesel engine using hydrogen as the fuel. Moreover, a spark ignition model built by C++ program was incorporated into the AVL FIRE® software to simulate the hydrogen ignition behavior. The model was validated by the experimental results and employed to examine important parameters that have significant effects onthe engine performance. The simulation results show that the variations of peak in-cylinder pressure, heat release rate, brake thermal efficiency, ignition delay, combustion duration, and NO emissions reasonably agree with the experimental findings. In order to reduce NOx emission an exhaust gas recirculation (EGR) system has been employed in the engine model.The computations are consistent with the hypothesis that gas cylinder temperature decreases with adding EGR and that the decrease in gas cylinder temperature results in the reduction in NO emissions.*

Keywords*: detailed chemical kinetics for hydrogen, AVL FIRE®, spark ignition engine, hydrogen engine and exhaust gas recirculation (EGR), emissions.*

Date of Submission: 16-01-2019 Date of acceptance:02-02-2019

I. Introduction

Due to the rapid depletion of fossil fuels and their detrimental effect on the environment, many researchers have put considerable effort into developing and introducing alternative transportation fuels to replace conventional fuels, such as gasoline and diesel [1]. Hydrogen is one of the most promising alternative fuels for internal combustion (IC) engines due to its positive effects and its limited number of negative effects. In the absence of carbon and sulfur the hydrogen-operated engine produces water as its main combustion product. It does not produce significant amounts of carbon monoxide (CO), hydrocarbon (HC), smoke, sulphur oxides (SO_X), or carbon dioxide (CO_2). The only undesirable emissions are the nitrogen oxides (NO_X), specifically nitric oxide (NO) and nitrogen dioxide (NO_2). This high level of NO_X is due to the high combustion temperature in hydrogen-fuelled engines[2].Some of the important properties of hydrogen are given in Table 1 [3-6].

Hydrogen has a wide flammability range in comparison with all other fuels. Hydrogen also has a high flame speed. This means that hydrogen engines can more closely approach the thermodynamically ideal engine cycle. The higher flame speed results in a high rate of pressure rise in hydrogen fueled engines; therefore, combustion is almost instantaneous. The higher flame speed and wider flammability limits make hydrogen engines more efficient in stop-and-start driving. The high burning rate of hydrogen produces high pressures and temperatures during combustion in chamber combustion when operating in near-stoichiometric mixtures. This may lead to high exhaust emissions of oxides of nitrogen.

Hydrogen has very low ignition energy. The ignition energy required to ignite the hydrogen is very low, which allows hydrogen engine to ignite lean mixtures and ensures prompt ignition. However, the low ignition energy leads to uncontrolled pre-ignition/backfire problems [7, 8]. Hydrogen's high diffusivity quickly spreads fuel leaks, therefore reducing the explosion hazards associated with hydrogen engine operation.

Hydrogen has a very low density. This means that the hydrogen engine needs a tank of very large volume to store enough hydrogen to give the vehicle an adequate driving range.

Hydrogen's high auto-ignition temperature (858°K) makes hydrogen more suitable as a fuel for spark ignition (SI) engines [9–12] than for IC engines. However, the hydrogen cannot be used directly in a diesel engine, because it is very difficult to ignite hydrogen just by the compression process, due to its auto-ignition temperature (858°K) being so much higher than that of diesel fuel (525°K) [13]. Therefore, some sources of ignition (spark plugs, glow plugs, or pilot fuel [14-24]) have to be generated inside the combustion chamber to ensure the ignition of hydrogen.

Today, Computational Fluid Dynamics (CFD) has become an essential tool in the process of designing and developing engineering devices. In the past few decades, the 3D CFD code has become a commonly used tool to gain a better knowledge about the combustion processes inside the engine cylinder. CFD offers successful assessment of newtechnologies, e. g., new fuel preparation methods, new combustion concepts, and/or alternative fuels. With the recent development of computer processors and the expansion of allowable memory, researchers and engineers are now able to integrate detailed chemical kinetics with a computational fluid dynamics (CFD) code to simulate IC engines.

Background and Motivation

To achieve the maximum advantages of hydrogen with the above distinctive properties, exhaustive research is required for the development of fuel-specific combustion and emission models. Advanced control approaches and operating strategies to reduce NOx emissions at high loads are also required. These efforts have the potential to produce more efficient and lower emission hydrogen engines that surpass the current fossil fuel-burning IC engines.

During the past few years, numerous researchers have made an effort to use hydrogen as fuel compression ignition engines[25]. Some researchers have used diesel as an ignition source to ignite hydrogen [19-22], and others have used glow plugs or spark plugs as an ignition source. Homan et al. [14] carried out experiments on a diesel engine converted for hydrogen operation without providing a timed ignition system. A glow plug and a multiple-strike spark plug were tested as ignition sources. It was found that glow plug ignition was an attractive way to operate hydrogen-fueled engines with direct cylinder injection late in the compression stroke. Welch et al. [16] performed hydrogen injection investigations using a glow plug for ignition assist and found that the use of hydrogen provided higher power than the same engine could provide on diesel. Wong [23] tried using a ceramic part as a glow plug to retain heat as the ignition source. Many statistical studies have focused on using three-dimensional computational fluid dynamics (CFD) tools to understand the in-cylinder flow field and mixing process [24, 26-31].Rakopoulos et al. [29, 30] have recently developed combustion model, which is incorporated in an in-house CFD code using RNG k-ε turbulence model for the simulation of a hydrogen spark-ignition engine. That model is composed of various sub-models used for the simulation of combustion of conventional fuels in SI engines; it has been adjusted for simulation of hydrogen combustion engine. They have investigated the combustion processes inside cylinder, especially with varying equivalence ratios. Kosmadakis et al. [31] have investigated the variation of EGR rates in that model in order to decrease the exhaust nitrogen oxides emissions.

Few studies have also focused on integrated chemical kinetics details with CFD code [32-34]. AVL FIRE® is one type of three-dimensional CFD engine simulation software. AVL FIRE® software has been widely used in predicting the performance of diesel engines. Some studies have investigated and reported on the integration of detailed diesel chemical kinetics with the AVL FIRE® CFD code [35,36].

In the present model, detailed chemical kinetic reactions for hydrogen oxidation with additional nitrogen oxidation reactions were combined with the AVL FIRE® CFD code using k-zeta turbulence model to run a hydrogen-fuelled diesel engine. Also, a spark ignition model was built using C++ programming and incorporated into the AVL FIRE® software to simulate the hydrogen ignition behavior.

An advantage of this model is the FIRE General Gas Phase Reactions Module was used for simulation of spark-ignition engines that run on either hydrogen fuel or conventional fuels, contrary to what it is done in most existing engines models.

Computational Method

AVL FIRE® presents a general species transport model to allow the implementation of a detailed kinetic model [35]. FIRE® solves species transport equations for aarbitrary number of chemical species. The species mass conservation equation is expressed as :

$$\frac{\partial(\rho w_i)}{\partial t} + \frac{\partial}{\partial x_k}(\rho(U_k - U_{\delta k})w_i) = \frac{\partial}{\partial x_k}\left(\left(\rho D_i + \frac{\mu}{\sigma_{ci}}\right)\frac{\partial}{\partial x_k}\right) + S_{w_i} \qquad (1)$$
$$S_{w_i} = r_i$$

Wherew_i is the mass fraction, S_{w_i} is the source term of species i by taking into account homogeneous chemical reactions,σ_{ci} is the stress tenser, and μ is the viscosity. Based on parameters extracted from a database, the physical properties (viscosity, density, specific heat, diffusion coefficient, thermal conductivity) shown in the equation above are calculated for each species and for gas mixtures by using the chemical kinetic databases (CHEMKIN™).

The chemistry effect (level of elementary reactions) is taken into account such that at the beginning of each CFD time step (Δt), a single zone reactor model is calculated for each computational cell. At the latest CFD time step for the properties (pressure, volume, temperature), the following conservation equations are integrated by the model for the time step (Δt), considering the volume cell as a function of time $\{V = V(t)\}$. The species conservation equation is computed using:

$$\rho \frac{\partial w_i}{\partial t} = M_i \omega_i \qquad (2)$$

Where M_i is the molecular weight of *i*th species, and ω_i is the molar species production rate. In this case, only the source term, S_{w_i}, is taken into account due to the homogeneity assumption. The energy conservation equation is expressed as:

$$\rho c_v \frac{\partial T}{\partial t} + \frac{P}{V}\frac{\partial V}{\partial t} = -\sum_{i=1}^{N_y} u_i M_i \omega_i \qquad (3)$$

On the left-hand side, the first term represents the temporal change of energy content, and the second term represents the volume work. The terms on the right-hand side represent the consideration of the change of inner energy due to production and consumption of chemical species. By using an interface to the CHEMKIN™ libraries, the molar species production rates, ω_i, can be calculated, and the source terms can be calculated by neglecting any effect of turbulence/mixing on the chemical reaction as follows:

$$r_i = \frac{\tau_{kin}}{\tau_{kin} + f\tau_{turb}} \frac{\rho^{n+1} w_i^{n+1} - \rho^n w_i^n}{\Delta t} \qquad (5)$$

$$\tau_{kin,i} = \Delta t \, \frac{\rho^{n+1} w_i^{n+1}}{\rho^{n+1} w_i^{n+1} - \rho^n w_i^n} \qquad (6)$$

$$\tau_{kin} = \max\left(\tau_{kin,f}, \tau_{kin,CO}\right) \qquad (7)$$

Where the superscripts n and n+1 indicate the first and the last values of the single zone reactor model. Keeping the source terms constant for the following CFD time step is the most important advantage of this approach because it makes the CFD simulation 100 percent conservative, fast, and valid.

The following approach considers the effects of both mixing and chemical kinetics by assuming that the reaction rate is determined via a kinetic time scale τ_{kin} (an equilibrium assumption under perfect mixed conditions) and turbulent time scale τ_{turb} (an eddy break up assumption). Furthermore, it assumes that the equilibrium concentration of the fuel is zero and the kinetic time scale is equal to the scale used for the fuel for all the species. By taking these assumptions into account, the above equation becomes

The turbulent time scale τ_{turb} can be calculated using the following:

$$\tau_{\text{turb}} = C_t \frac{k}{\varepsilon} \quad (8)$$

The variable *f* is a delay coefficient that uses to simulate the influence of turbulence on combustion after ignition has occurred [37] and can be calculated as:

$$f = \frac{1 - e^{-r}}{0.632} \quad (9)$$

$$r = \frac{w_{H_2O} - w_{H_2}}{1 - w_{N_2}} \quad (10)$$

In this study the k-zeta-f model was chosen. This model recently developed by Hanjalic, Popovac and Hadziabdic [38]. For IC-engine flows the k-z-f model leads to more accurate results than the much simpler two-equation eddy viscosity models of the k-e type by simultaneously exhibiting a high degree of numerical robustness. This model is based on Durbin's elliptic relaxation concept, which solves a transport equation for the velocity scales ratio $\zeta = \frac{\overline{v^2}}{k}$instead of the equation for $\overline{v^2}$[38]. The$\overline{v^2}$ is the velocity scale and k is the turbulence kinetic energy. Durbin's model is described in [39].The FIRE General Gas Phase Reactions Module was used to enable the simulations of kinetic problems.The detailed chemical kinetics for hydrogen was integrated with the AVL FIRE® multidimensional CFD code to convert a diesel engine to a hydrogen engine. The detailed chemical kinetic reactions for hydrogen consist of 20 steps with additional oxidation reactions involving nitrogen, [40]. The CHEMKIN chemistry solver was integrated into the AVL FIRE® code for solving the chemistry during multidimensional engine simulation. The AVL FIRE® code provides CHEMKIN the species and thermodynamic information of each computation cell, and the CHEMKIN utilities return the new species information and energy release after solving for the chemistry, the detailed chemistry modeling scheme shown in the figure 1.

User-function was applied to use the spark ignition model. A spark ignition model was built using C++ programming and incorporated into the AVL FIRE® software to simulate the hydrogen ignition behavior.The piston geometry and computational grid used for the simulations are shown in Figure 2. It was built up using the commercial CFD tool AVL ESEDiesel. The computational domain consists of one sectionof the modeled engine cylinder, which was used for simulations between inlet valve closing (IVC) and exhaust valve opening (EVO). This means that only the closed volume part of the engine cycle is computed. The mesh was composed of about 12960 computational cells with mesh size was 3.33 ×3.33×3.56 mm and nodes number 14167. The convergence criterion is either maximum number of iterations 60 or reduction of residuals as 0.01 whichever achieves first.

II. Results And Discussions

The operating conditions of the hydrogen IC engine modeled and simulated in this investigation were chosen similar to the independent study by Subramanian et al. [41] because their reported test conditions and experimental data were well documented. Specifications of the spark-ignition hydrogen engine used in this computational study are listed in Table 2.The initial operating conditions of engine are listed in Table 3.Two cases were selected to study engine combustion and to predict the in-cylinder emissions formation process. These selected cases were at brake power of 7.4 kW and 2 kW with equivalence ratio of 0.84 and 0.3 respectively.

Brake Thermal Efficiency

Variations of brake thermal efficiency with brake power are depicted in Fig. 3. The brake thermal efficiency increased as the brake power increased.The predicted brake thermal efficiency for two cases, at abrake power of 2 kW (ϕ = 0.3) and 7.4 kW (ϕ = 0.84), are in good agreement with the experimental data collected. The maximum brake thermal efficiency was nearly 30 % with brake power of 7.4 kW (ϕ = 0.84) compared to 19 % for brake power of 2 kW (ϕ = 0.3). The main reason of high brake thermal efficiency at high brake power is because at higher brake power outputs, flame speed increases as the equivalence ratio increases and therefore nearly constant volume combustion is achieved with hydrogen, which results in higher brake thermal efficiency.Ignition timing also had a significant influence on the thermal brake power. For the case with an equivalence ratio of 0.84, the spark time was 5 BTDC (Before Top Dead Center), while with an equivalence ratio of 0.3, it was 42 BTDC.With an equivalence ratio of 0.3, the spark time occurred too early BTDC. Hence a

large amount of gas was burned while the piston was still going up as illustratedin the Fig. 14, thisprocess will contribute to decrease the network produced and hence leading to reduction in the efficiency.

In-Cylinder Pressure

Cylinder pressure variations with crank angle as well as with relative cylinder volume are shown in Figures 4 and 5 for an equivalence ratio of 0.84. The peak pressure for the hydrogen engine in the present model was approximately 55bar, fairly comparable with the corresponding experimental values of 50 bar [41]. The P-V diagramalso indicatesthat the heat addition process in the hydrogen engine takes place at a nearly constant volume, similar to the Otto cycle, due to a much faster combustion.

Figure4also illustrates the predicted in-cylinder pressure as a function with a crank angle foran equivalence ratio of 0.3. At thisequivalence ratio, the peak pressure was lower than that at anequivalence ratio of 0.84. As the equivalence ratio (or brake power) increased, both the peak pressure and the rate of pressure increased as depicted in Fig. 6. The peak pressure was found to increase almost linearly with equivalence ratio (or brake power). This is because the flame speed increasedas the equivalence ratio (orbrake power) increasedand the time required to complete the combustion decreased.The predicted peak pressure was in good agreement with the experimental data collected at a brake power of 2 kW ($\phi = 0.3$). Several simple differences occurred at a maximum brake power of 7.4 kW ($\phi = 0.84$).

A contour plot of in-cylinder pressure during the combustion process is illustrated in Fig. 7. At an equivalence ratio of 0.3(at 2 kW), the peak pressure occurred at 8^o ATDC (After Top Dead Center)compared to 6^o ATDC forequivalence ratio of 0.84 (at 7.4 kW).The pressure rate at an equivalence ratio of 0.84 was (4 bar/deg) higher(0.8 bar/deg) than that at an equivalence ratio of 0.3, as shown in the figure. At TDC (Top Dead Center), the pressure was about 2.96 bar for equivalence ratio of 0.3 (2 kW), while it was 2 bar forequivalence ratio of 0.84 (7.4 kW) as shown in figure. Immediately after TDC, the rate of pressure rises drastically for case of equivalence ratio of 0.84and becomes higher than that at equivalence ratio of 0.3. Than after crank angle of 8^o ATDC and 6^o ATDC, the pressure start to decline during expansion stroke for equivalence ratio of 0.3 and 0.84 cases respectively. The pressure rate agreed with Subramanian'sexperiments [41].

Variation of Heat Release With Crank Angles

Fig. 8 illustrates the predicted heat release ratesas a function of crank angle for the maximum equivalence ratio of 0.84. Thepredicted peak heat release in the hydrogen engine was 83 J/deg. The results indicate that hydrogen's faster burning speed produces a relatively high rate of heat release in a small time interval.Several of the simple divergences that occurred in predicting the heat release rate (HRR) could have been caused either bydeficiencies in the computer models or differences in the boundary conditions between the simulations and the experiments.

Emissions

Nitric oxide is the only emission produced by hydrogen engines. Any carbonemissions (e.g., CO, CO_2 and HC) will be very little. Thus they are omitted in emission discussions.Fig. 9 illustrates both the predicted and the measured NO emissions as a function of brake power (orequivalence ratio). These NO emissions were almost negligible below an equivalence ratio of 0.55 (or 5 kW). When the equivalence ratio increased beyond this value, suddenly the NO emission rapidly increase and reach a peak value of approximately 9500 ppm at an equivalence ratio of 0.84 (at 7.4 kW). ThisNO was formed primarily as a result of the following reactions:

$$N_2O + O = N_2 + O_2 \quad (R1)$$
$$N_2O + O = NO + NO \quad (R2)$$
$$N_2O + H = N_2 + OH \quad (R3)$$
$$N_2O + OH = N_2 + HO_2 \quad (R4)$$
$$N_2O + M = N_2 + O + M \quad (R5)$$

The other path to NO_x formation can be described by reactions R6, R7, and R8, typically known as the extended Zel'dovich mechanism:

$$N_2 + O = N + NO \quad (R6)$$
$$N + O_2 = NO + O \quad (R7)$$
$$N + OH = NO + H \quad (R8)$$

Normally, these three reactions are only important at high temperatures because radicals O and OH are created in high temperature gases.

Fig.10illustrates the NO emission at an equivalence ratio of 0.3. Here the NO reaches its maximum value and is essentially "frozen" at that value, and does not change during the remainder of the expansion stroke. The CFD also confirmed that, as the equivalence ratio decreased, the oxygen concentrations increased.

When the mixture was leaned (ϕ = 0.3), the oxygen concentrations increased and the in parallel cylinder temperature decreased. Thus, the NO emissions decreased. These emissions are influenced, primarily, by a reduction in temperature rather than the availability ofO_2.

Fig. 11depicts the NO emissions at an equivalence ratio of 0.84. Herethe peak in NO occurs near the spark-plug where the local temperature is very high (at flame region). It then begins to decline as the crank angle increases during expansion stroke. As result to decline in-cylinder temperature, the rate of NO decomposition rapidly decreases, so after crank angle of 50 AIT (After Ignition Time), the NO kinetics is effectively frozen, that because after 50° AIT, the rates of (R6), (R7), and (R8) become small and the concentration of NO remains almost constant during the remainder of the expansion stroke.

An exhaust gas recirculation (EGR) system was used to reduce NO emissions. For hydrocarbon fuels, the EGR rate is generally calculated from a molar CO2 balance. For hydrogen engines, however, this cannot be used as no CO2 emissions occur. Three methods are available that can calculate the amount of EGR ina hydrogen engine[42]. The first is based upon a volume balance in the mixing section of exhaust gases and fresh air. The second method uses a molar balance of O_2 and third one uses a molar balance of H_2O. The third method was used in this study.

The information in Fig. 12 suggests that at fullbrake power, the peak NO was7500 ppm and 288 ppmbyadding 5 % EGR and 15 % EGR respectively, compared to 9500 ppm without EGR. It is generally known that there are two reasons to reduce NO by EGR. The first of them is the reduction of combustion temperature. The addition of exhaust gases to the intake charge increases the amount of combustion-accompanying gases, which in turn increases the heat capacity and lowers the cylinder combustion temperature. The second effect is the reduction of oxygen concentration in the intake charge, which restrains the generation of NO.

The CFD results are consistent with the hypothesis that both gas cylinder temperature and oxygen concentrations decreasewhen EGR is added.The decrease in gas cylinder temperature and oxygen concentration results in the reduction in NO emission as shown in fig. 13. The temperature contour also indicates that with 15 % EGR, the temperature near the combustion cylinder's sides was very low. This low temperature may be due to the slow propagation of the flame with EGR level. The simulations of NO emissions conducted in this study agree with the experimental data of Subramanian et al. [41] on a single hydrogen engine. It alsoagree with simulations conducted with GT-power software and presented byVudumuet al. [42].Finally, should also be noticed that the oxygen concentration in the exhaust gas was gradually reduced as the equivalence ratio for hydrogen engine was increased.

Ignition Delay And Combustion Duration

The ignition delay is defined as the length of time (or crank angle interval) between instant of spark and the inflammation of the air-fuel mixture (release of the first 5 percent of total heat energy). The combustion duration is the crank angle covered for 5 to 90 percent of the total heat release.

The CFD results confirm that the ignition delay decreases as the equivalence ratio increases, as depicted in fig. 14. It can be observed that operating at an equivalence ratio of 0.3 (lean mixtures), the ignition delay was 12 crank angles compared to 6 crank angles at equivalence ratio of 0.84. This is may be due to increase in energy input and mixture reactivity with increasing equivalence ratio, which advances the ignition time.

Figures (7) and (8) indicate that the combustion duration for the two cases. At an equivalence ratio of 0.3 (Fig. 7), the combustion duration was longer than the combustion duration at an equivalence ratio of 0.84 (Fig. 8). At an equivalence ratio of 0.3, the flame covered the entire cylinder at a crank angle of 67^o AIT (see Fig. 7), however, for an equivalence ratio of 0.84, the flame covered the entire cylinder at 30^o AIT (see Fig. 8). This might be due to that the less thermal energy liberated from the leaner mixture which increases the ignition delay and slows the flame propagation. This results were agreed with observations of Rakopoulos et al. [29, 30]. The combustion duration also increased as the EGR level increased. As shown in Fig 12 that for the 5 % EGR level case, the flame has covered the whole combustion chamber at crank angle of 30 AIT. At that moment the NO mass fraction has its peak value, and starts to decrease afterwards. However with the 15 % EGR level case, the burning velocity is very low, since at crank angle of 30 AIT, the flame still propagates. This results were agreed with observations of Kosmadakis et al. [31].

III. Conclusions

The CFD simulation work carried out using AVL FIRE software for an IC Engine fueled with hydrogen gas with varying brake power resulted the following conclusion:

- Model results showed good agreements with the experimental results for peak cylinder pressure, heat release, brake thermal efficiency, NO emission, ignition delay, and combustion duration.

- NO emissions were negligible at lower equivalence ratios but, beyond an equivalence ratio of 0.55, NO sharply increased.
- The CFD results confirmed that gas cylinder temperature decreased with EGR and that the decrease in gas cylinder temperature resulted in the reduction in NO emissions.
- The combustion duration and ignition delay became longer as the mixture was made leaner.

Thus present model investigation on a single cylinder hydrogen engine has proved to be viable approach to study combustion parameters and emissions in-cylinder for hydrogen fuelled IC engine. This is expected to lead to improved designs of hydrogen engines.

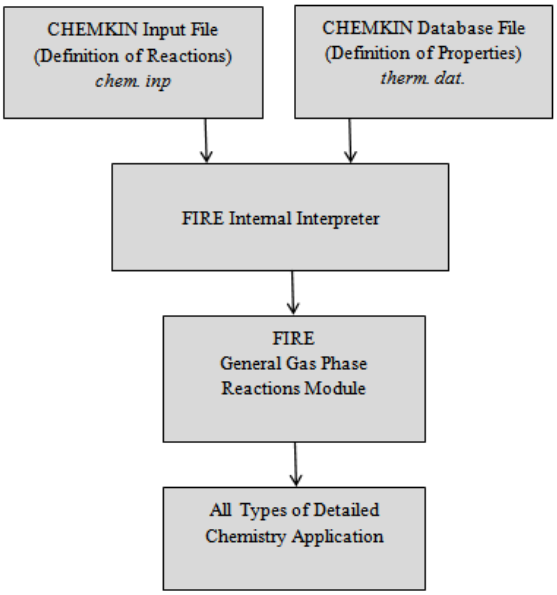

Figure 1 detailed chemistry modeling scheme

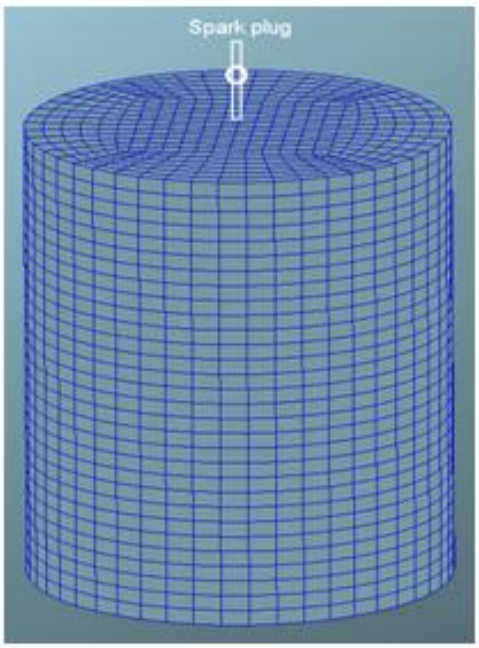

Figure 2 Computational mesh (50 sectors, 12960 cells)

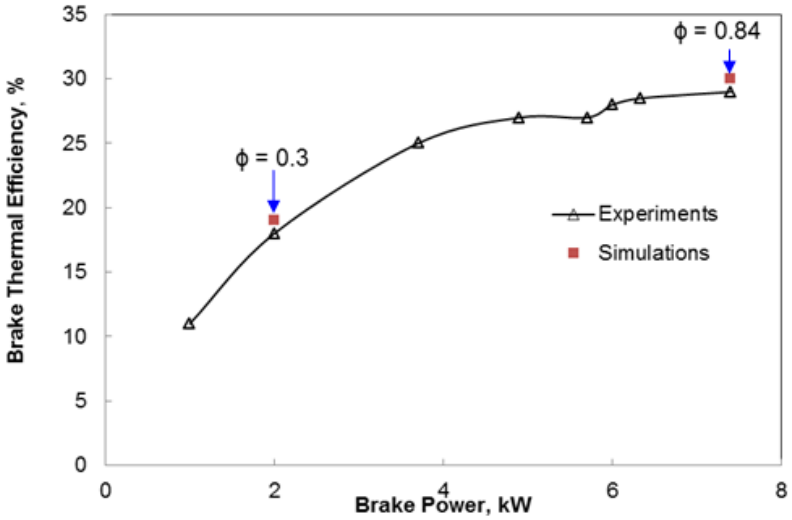

Figure 3 Variation of brake thermal efficiency with brake power

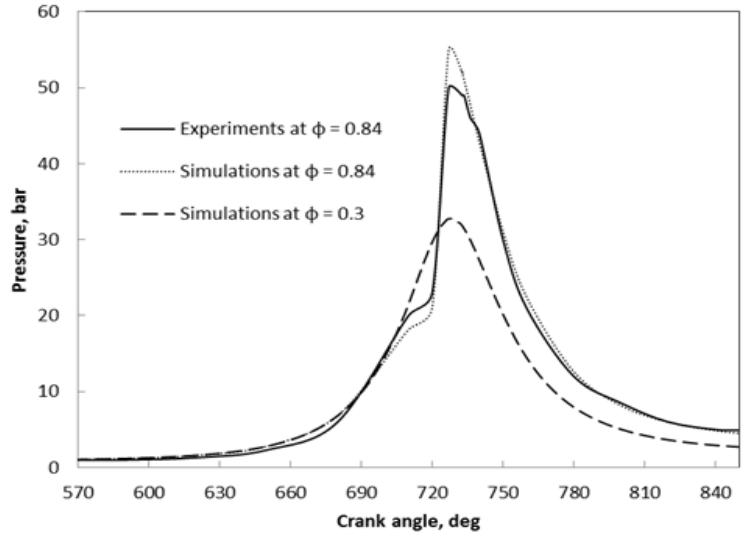

Figure 4 Variation in cylinder pressure as crank angle varies

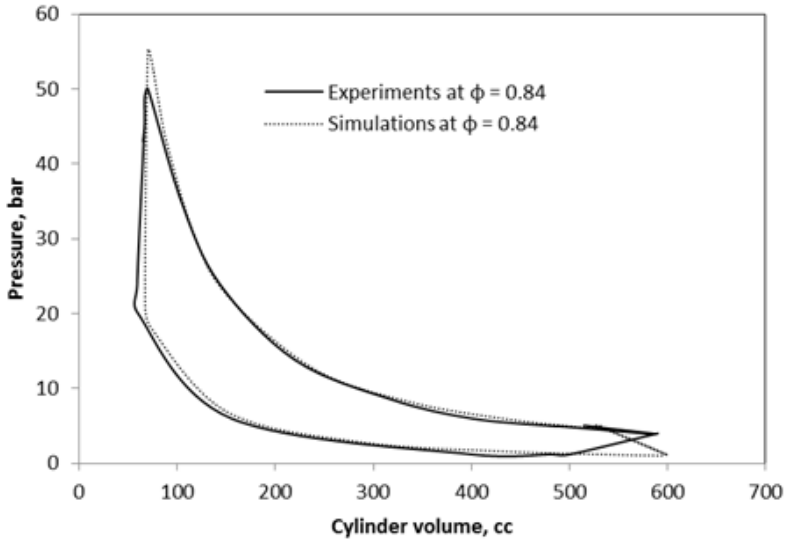

Figure 5 Cylinder pressure with volume

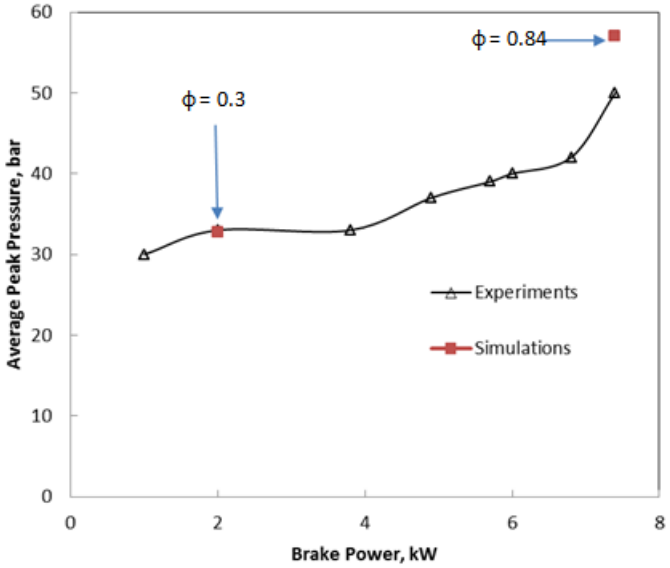

Figure 6 Variation of peak cylinder pressure with brake power

	At equivalence ratio of 0.3 (2 Kw)	At equivalence ratio of 0.84 (7.4 Kw)
TDC	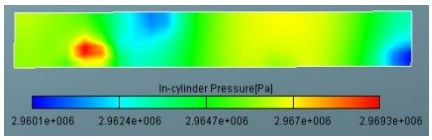	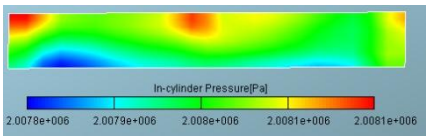
6^{O} ATDC	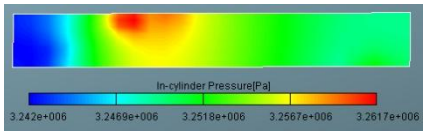	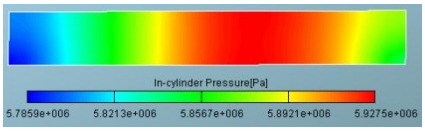
8^{O} ATDC	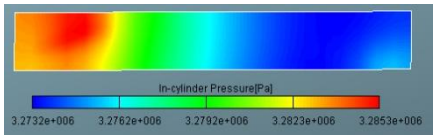	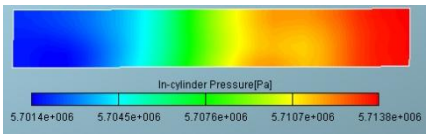
10^{O} ATDC	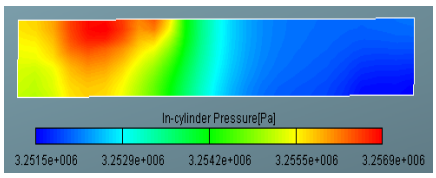	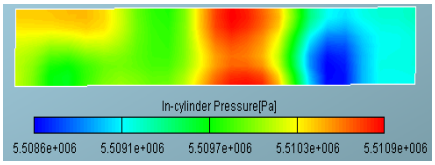

Figure 7 pressure contour during combustion process

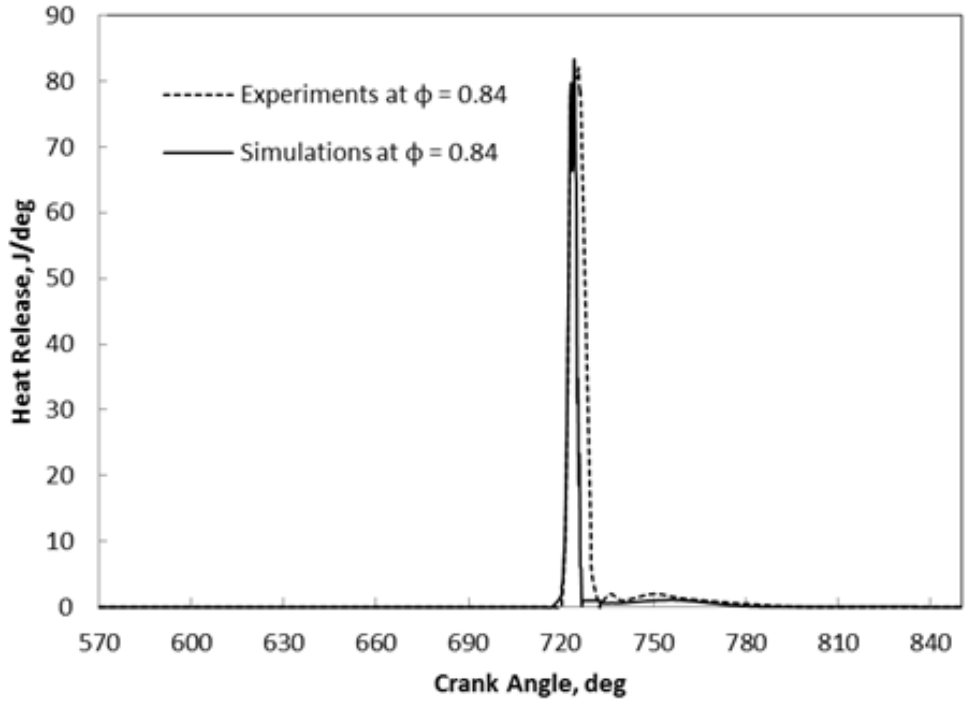

Figure 8 Variation in heat release as crank angle varies

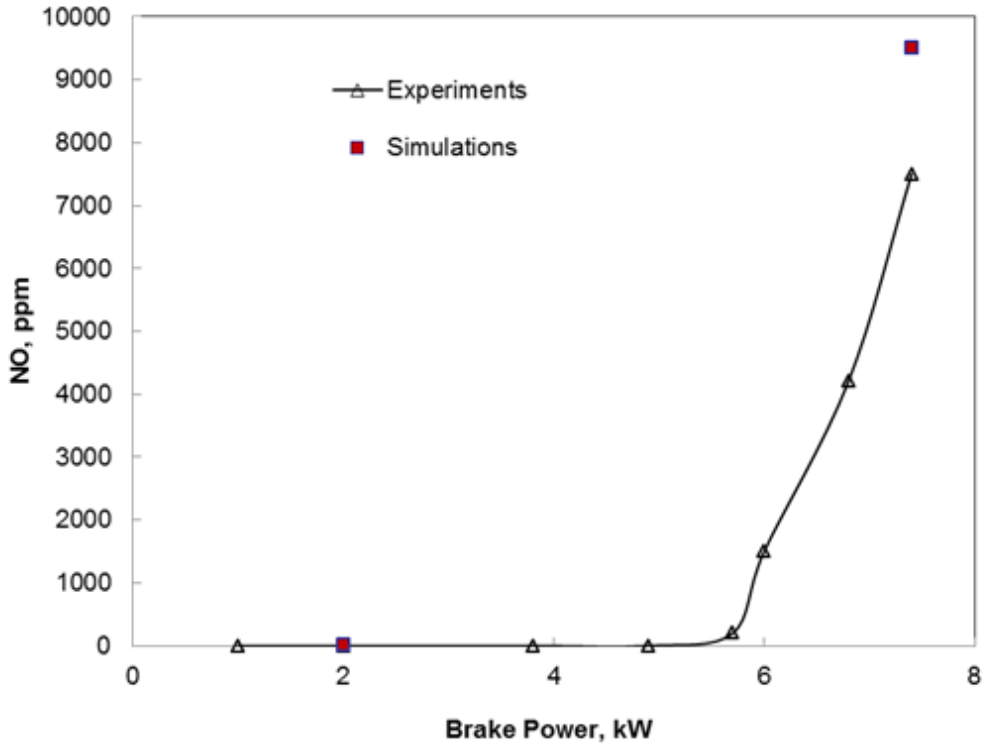

Figure 9 Variations of NO emission with brake power

Crank angle	NO [-]	Temperature, K	Oxygen mass fraction
47 AIT	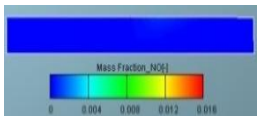	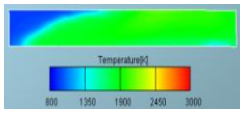	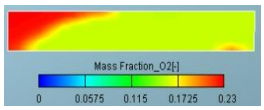
67 AIT	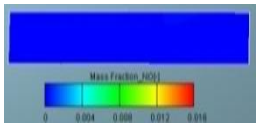	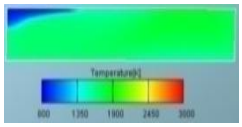	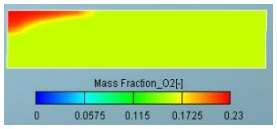
87 AIT	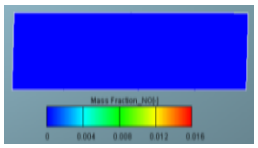	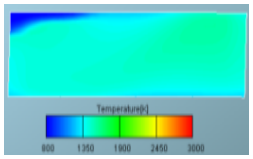	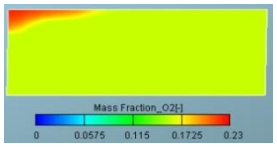
97 AIT	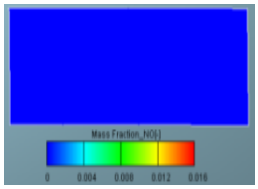	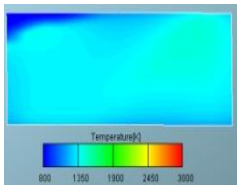	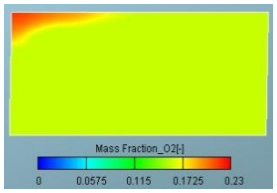

Figure 10 NO , O2 and temperature contour during combustion process at equivalence ratio of 0.3

Crank angle	NO [-]	Temperature, K	Oxygen mass fraction
10 AIT	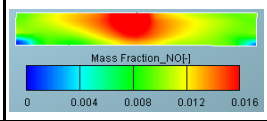	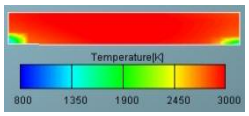	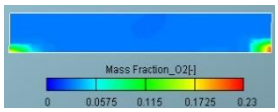
30 AIT	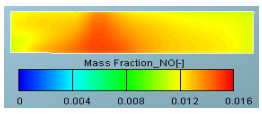	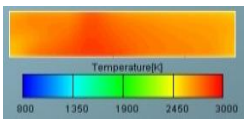	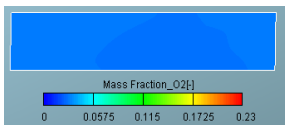
50 AIT	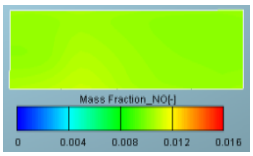	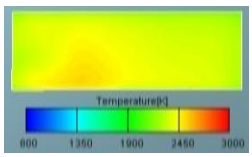	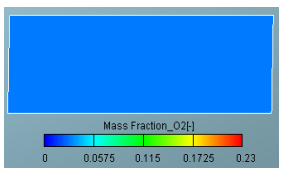
60 AIT	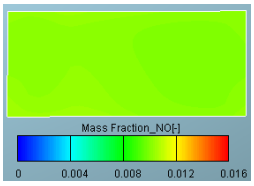	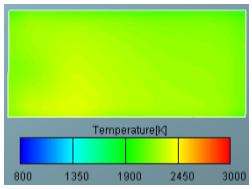	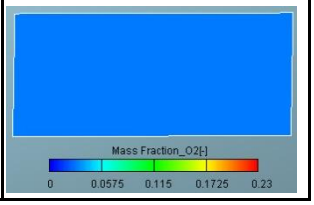

Figure 11 NO , O2 and temperature contour during combustion process at equivalence ratio of 0.84

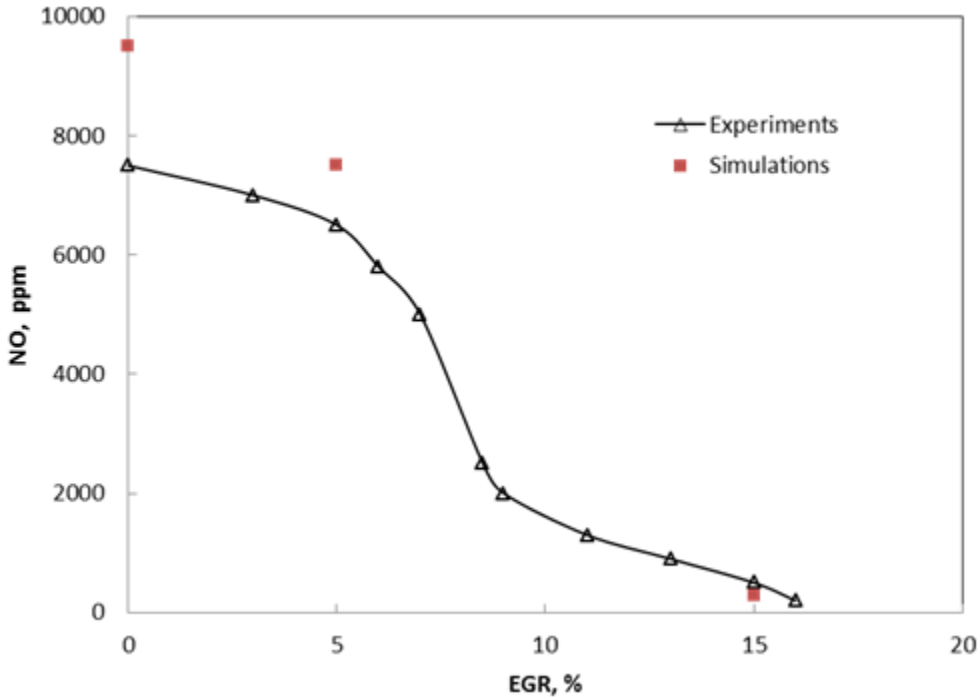

Figure 12 Variation of NO emissions with EGR

Crank angle	5 % EGR	15 % EGR
10 AIT	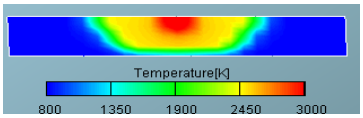	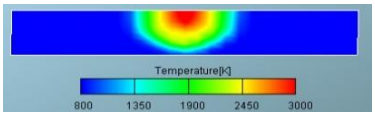
	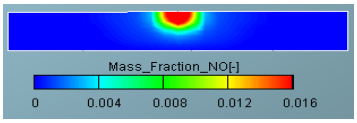	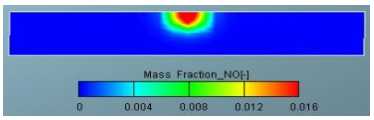
30 AIT	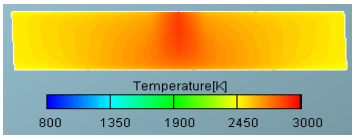	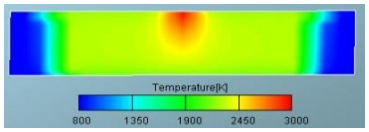
	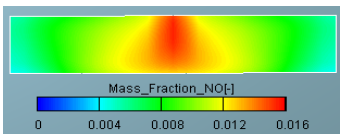	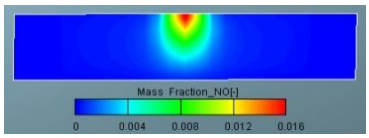

Figure 13 Temperature and NO mass fraction contour during combustion process with 5 % and 15 % EGR at full brake power

Equivalence ration = 0.3		Equivalence ration = 0.84	
Crank angle, deg.	Ignition delay	Crank angle, deg.	Ignition delay
Ignition time 42 BTDC	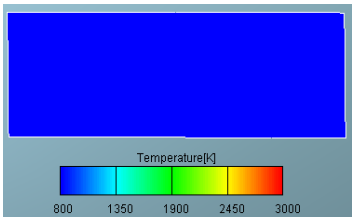	Ignition time 5 BTDC	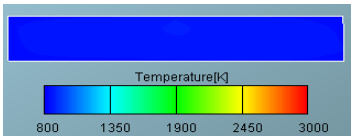
20 BTDC (12 AIT)	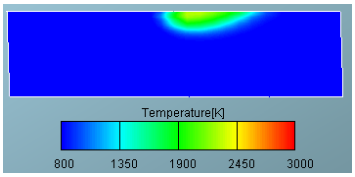	1 ATDC (6 AIT)	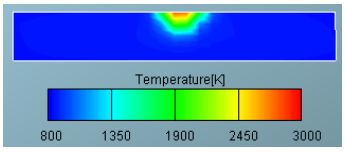

Figure 14 Temperature contour during combustion process shows the ignition delaywithequivalence ratios

Table 1 Properties of hydrogen in comparison with diesel and gasoline.

Properties	**Hydrogen**	**Gasoline**	**Diesel**
Auto igntition temperature (K)	858	550	530
Minimum ignition energy (mJ)	0.02	0.24	-
Flammability limitsin air (vol. %)	4-75	1-7	-
Net heating value (MJ/kg)	119.9	44.79	42.2
Stoichiometric air/fuel (mass)	34.3	14.7	14.5
Density at ambient(kg/m^3)	0.083	730	824
Quenching gap in NTP air(cm)	0.064	0.2	-
Stoichiometric flame speed (m/s)	2.65-3.25	0.37-0.43	0.3

Table 2Specifications of the IC engine modeled

Fuel	Hydrogen
Number of cylinders	1
Bore × Stroke	85 × 95 mm
Displacement volume	530 cm^3
Compression ratio	9:1
Engine speed	2500 rpm

Table 3 Initial operating conditions of engine

Start angle	540
End angle	850
Piston surface temperature	423 K
EGR %	15 %
Swirl ratio	1.2
Turbulence model	k-zeta-f model
Turbulence kinetic energy	2 m^2/s^2
Turbulence length scale	0.0045 m
Initial temperature	330 K
Initial pressure	1 bar
Computational time step	0.25 deg.

Acknowledgments

The authors are thankful to the Libyan government for financial support and Missouri University of Science and Technology and Tobruk University for providing the necessary facilities. Also, the authors would like to give their sincere thanks to Jun Li from AVL Advanced Simulation Technology for his support with the computations.

References

[1]. Verhelst, S. Recent progress in the use of hydrogen as a fuel for internal combustion engines.*Int. J. Hydrogen Energy***2014** (39) 1 0 7 1-1 0 8 5.

[2]. Jongtai, L.; Kwangju, L.; Jonggoo, L.;Byunghoh, A. High power performance with zero NOx emission in a hydrogen-fueled park ignition engine by valve timing and lean boosting.*Fuel* **2014** (128) 381-389.

[3]. BarretoL., MakihiraA. The hydrogen economy in the 21st century: a sustainable development scenario. *Int. J. Hydrogen Energy***2003** (28), 267-284.

[4]. Subramanian, V.; Mallikarjuna, JM.; Ramesh, A. Performance, emission and combustion characteristics of a hydrogen fueled SI engine-an experimental study. **2005***SAE Technical Paper*., pp. 26-349.

[5]. Verhelst, S.; Wallner, T. Hydrogen-fueled internal combustion engines. *Prog Energy Combustion Science.***2009**35, pp. 490-527.

[6]. Peter, Van Blarigan. Advanced Hydrogen Fueled Internal Combustion Engines*Energy Fuels***1998**, 12 (1), pp 72–77.

[7]. White, C.; Steeper, R.; Lutz, A. The hydrogen-fueled internal combustion engine: a technical review. *Int. J. Hydrogen Energy***2006** (31) 1292-305.

[8]. Verhelst, S.; Sierens, R.; Verstraeten, S. A critical review of experimental research on hydrogen fueled SI engines. *SAE Technical Paper***2006**pp. 01-0430.

[9]. Mathur, HB.; Khajuria, P. Performance and emission characteristics of hydrogen fuelled spark ignition engine. *Int. J. Hydrogen Energy***1984** 729–35.

[10]. Karim, GA. Hydrogen as a spark ignition engine fuel. *Int. J. Hydrogen Energy***2003** (28) 569–77.

[11]. Mohammadi, A.; Shioji, M.; Nakai, Y.; Ishikura, W.; Tabo, E. Performance and combustion characteristics of a direct injection SI hydrogen engine. *Int. J. Hydrogen Energy* **2007 (**32) 296–304.

[12]. Kawahara, N.; Tomita, E. Visualization of auto-ignition and pressure wave during knocking in a hydrogen spark-ignition engine. *Int. J. Hydrogen Energy***2009** (34)3156–63.

[13]. Das, LM. Hydrogen engine: research and development (R&D) programmes in Indian Institute of Technology (IIT), Delhi. *Int. J. Hydrogen Energy***2002** (27)953–65.

[14]. Homan, H; Reynolds, R.; De Boer, P.; McLean, W.J. Hydrogen-Fueled Diesel Engine Without Timed Ignition. *Int. J. Hydrogen Energy***1979**(4) 315-325.

[15]. Naber, J.; Siebers, D.;, "Hydrogen Combustion under Diesel Engine Conditions," International Journal of Hydrogen Energy., **1998**23(5)363-371.

[16]. Welch, A.; Wallace, J.; Performance Characteristics of a Hydrogen-Fueled Diesel Engine with Ignition Assist. *In Society of Automotive Engineers, International Fuels and Lubricants Meeting & Exposition,***1990** October. URL http://papers.sae.org/902070.

[17]. Furuhama, S.; Kobayashi, Y. Development of hot surface ignition hydrogen injection two-stroke engine. *Proc. Fourth World Hydrogen Energy Conference***1982** pp. 3.

[18]. Furuhama, S.; Fukuma, T. High output power hydrogen engine with high pressure fuel injection, hot surface ignition and turbocharging. *Int. J. Hydrogen Energy***1986** 11, pp. 399-407.

[19]. Adrian, B.; Cristian. Effects of Air-Hydrogen Induction on Performance and Combustion of a Diesel Engine. *Int. J. ASE*2011-24-0094

[20]. Saravanan, N.; Nagarajan, G. Performance and emission study in manifold hydrogen injection with diesel as an ignition source for different start of injection. *Renewable Energy***2009**34, pp. 328-334.

[21]. Saravanan, N.; Nagarajan, G.;Narayanasamy, S. An experimental investigation on DI diesel engine with hydrogen fuel. *Renewable Energy***2008**33, pp. 415-421.

[22]. Saravanan, N.; Nagarajan, G. Experimental Investigation in Optimizing the Hydrogen Fuel on a Hydrogen Diesel Dual-Fuel Engine. *Energy Fuels***2009**, 23 (5), pp 2646–2657.

[23]. Wong, JKS., "Compression ignition of hydrogen in a direct injection diesel engine modified to operate as a low-heat rejection engine. *Int. J. Hydrogen Energy***1990**15, pp. 507–14.

[24]. Horng-Wen, W.; Zhan-Yi, W. Investigation on combustion characteristics and emissions of diesel/hydrogen mixtures by using energy-share method in a diesel engine.*Applied Thermal Engineering***2012** (42) 154-162

[25]. Lee,K.;Kim,Y.R.Feasibility of compression ignition for hydrogen fueled engine with neat hydrogen-air pre-mixture by using high compression. *Int. J. hydrogen energy***2013** (38) 255-264.

[26]. Rakopoulos, CD.; Kosmadakis, GM.; Pariotis, EG., "Evaluation of a new computational fluid dynamics model for internal combustion engines using hydrogen under motoring conditions. *Energy***2009**, 12, pp. 2158-66.

[27]. Arash, H.; Pavlos, A. Computational Study of Hydrogen Direct Injection for Internal Combustion Engines. *SAE paper*, **2013**-01-2524.

[28]. Zhenzhong, Y.; Aiguo, S.; Fei, W.; Nan, G., "Research into the formation process of hydrogenair mixture in hydrogen fueled engines based on CFD. *Int. J. Hydrogen Energy***2010** (35) 3051-7.

[29]. Rakopoulos, CD.;Kosmadakis, GM.;Pariotis, EG. Evaluation of a combustion model for the simulation of hydrogen sparkignition engines using a CFD code. *Int. J. Hydrogen Energy***2010**;35(22):12545-60.

[30]. Rakopoulos, CD.;Kosmadakis, GM.; Demuynck, J.;Paepe, M.; Verhelst, S. A combined experimental and numerical study of thermal processes, performance and nitric oxide emissions in a hydrogen-fueled spark-ignition engine. *Int. J. Hydrogen Energy***2011**;36(8):5163-80.

[31]. Kosmadakis, GM.;Rakopoulos, CD.; Demuynck, J.; Paepe, M.;Verhelst, S. CFD modeling and experimental study of combustion and nitric oxide emissions in hydrogen-fueled spark-ignition engine operating in a very wide range of EGR rates. *Int. J. Hydrogen Energy***2012**;(37) 10917-10934.

[32]. Vincent, K.; Adle`ne, B.Modelling of combustion and nitrogen oxide formation in hydrogen-fuelled internal combustion engines within a 3D CFD code. *Int. J. of Hydrogen Energy***2008**(33)5083-5097.

[33]. Pitsch, H.; Peters, N., Three-Dimensional Modeling of NOx and Soot Formation in DI-Diesel Engines Using Detailed Chemistry Based on the Interactive Flamelet Approach. *SAE Paper***1996** 962057.

[34]. Wang H.; Mingfa Y.; Reitz, R.Development of a Reduced Primary Reference Fuel Mechanism for Internal Combustion Engine Combustion Simulations. *Energy Fuels***2013**, 27, 7843−7853.

[35]. Priesching, P.; Wanker, R., "Detailed and Reduced Chemistry CFD Modeling of Premixed Charge Compression Ignition Engine Combustion. *Int. Multidimensional Engine Modeling User's Group Meeting***2003**.

[36]. Khairallah, H.;Koylu,U. Combustion simulation of hydrogen-fuelled diesel engines using detailed chemical kinetics. *ASME*, IMECE**2013**-65194

[37]. Kong, S.; Marriott, C.; Reitz, R.; Christensen, M. Modeling and Experiments of HCCI Engine Combustion using Detailed Chemical Kinetics with Multidimensional CFD. Int. J. *SAE Paper***2001**-01-1026, 2001.

[38]. Hanjalic,K.;Popovac,M.;Hadziabdic, M. A robust near-wall elliptic relaxation eddy-viscosity turbulence model for CFD. *Int. J. Heat and Fluid Flow*, **2004** vol. 25, pp. 1047–1051.
[39]. Durbin, P. Near-wall turbulence closure modellingwithout damping functions. *Theoretical and Computational Fluid Dynamics*,1991 vol. 3, pp. 1–13.
[40]. https://github.com/OpenCFD/OpenFOAM1.7.x/blob/master/tutorials/combustion/dieselFoam/aachenBomb/chemkin/chem.inp_15.
[41]. Subramanian, V.; Mallikarjuna, J.; Ramesh, A., Performance, emission and combustion characteristics of a hydrogen fueled SI engine-an experimental study. *SAE Technical Paper***2005**pp. 26-349.
[42]. Verhelst, S.;Vancoillie, J. Setting a best practice for determining the EGR rate in hydrogen internal combustion engines. *Int. J.hydrogen energy***2013** (38) 2490-2503.
[43]. VudumuS.; Koylu, U Computational modeling, validation, and utilization for predicting the performance, combustion and emission characteristics of hydrogen IC engines. *Energy* 36 (**2011**) 647-655.

Hassan A. Khairallah. "Numerical Study of In-cylinder Combustion Characteristics and Emission of Hydrogen IC Engine Using a 3D Model with Chemical Kinetics ." IOSR Journal of Mechanical and Civil Engineering (IOSR-JMCE) , vol. 16, no. 1, 2019, pp. 38-52